

3D wave-ray traveltimes tomography for near-surface imaging

Long He*, Wei Zhang, Jie Zhang, University of Science and Technology of China (USTC)

Summary

First arrival traveltimes tomography is an appealing technique for near surface imaging, because it is efficient and it can handle complex velocity structures. However, since raytracing is applied in the approach with the assumption of infinite high frequency, it sometimes cannot justify the resolution of tomographic solution, particularly for small and thin structures. On the other hand, waveform inversion does honor resolution associated with data frequency, but it is very time consuming. We intend to incorporate wave resolution in the inversion while maintain the efficiency of the first arrival traveltimes tomography. This involves the use of the first Fresnel zone along raypath for sensitivity during traveltimes inversion. Numerical experiments indicate that an approximation to the first Fresnel zone should be sufficient. This method establishes a stepping stone between a ray-based traveltimes tomography and the full waveform tomography.

Introduction

Near-surface velocity structures imaging is an important and routine exercise in seismic data processing. Many seismic imaging methods have been developed to handle various situations. Among the current near-surface imaging approaches, the nonlinear first-arrival traveltimes tomography (Zhang and Toksoz, 1998) is stable, producing a long-wavelength structure solution (He et al., 2011). However, the traveltimes tomography also suffers from an obvious drawback that it adopts the infinite high frequency approximation in both forward modeling and inversion, which assumes seismic wave propagating in medium along a thin ray. Real seismic waves do not contain infinite high frequency but are band-limited signals, and the seismic wave propagation is influenced not only by the structure along the thin ray, but also by the structure in the vicinity of the ray (Cerveny and Soares, 1992). The finite-frequency nature of the seismic wave leads to the demand of the wave-equation traveltimes tomography (Luo and Schuster, 1991) and full waveform inversion (Tarantola, 1984). But such wave-equation techniques are computationally expensive. The finite-frequency effect can also be approximated by expanding sensitivity kernel only along the ray to sensitivity kernel occupying the entire first Fresnel zone (Vasco et al., 1995). We call this first Fresnel zone as wave-ray zone in this study. Husen and Kissling (2001) applied the Fresnel zone feature to global seismology tomography, Watanabe et al., (1999) and Ke et al., (2007) applied this method to 2D traveltimes

tomography and 3D traveltimes tomography in a small model scale.

In this study, we propose to combine the wave-ray theory into 3D nonlinear first-arrival traveltimes tomography. This approach accounts for finite frequency information in the inversion, and it makes more sense physically than conventional ray-based traveltimes tomography. Result derived by this wave-ray tomography method is more realistic than that obtained by the first-arrival traveltimes tomography. Compared with other similar Fresnel tomography or wave-ray tomography algorithms (Watanabe et al., 1999; Ke et al., 2007), our method employs the paraxial approximation (Dahlen et al., 2000) to construct an approximate Fresnel zone of each shot-receiver pair by single raytracing calculation rather than calculating a precise one, thus, it avoids extensive raytracing calculations for each receiver and is more efficient.

Fresnel zone and estimated wave ray zone

Cerveny and Soares (1992) defined the first Fresnel zone for a given shot-receiver pair in terms of traveltimes t_{SP} , t_{RP} and t_{SR} ,

$$|t_{SP} + t_{RP} - t_{SR}| \leq \frac{T}{2} \quad (1)$$

where t denotes the seismic traveltimes between two specific subscript points, S denotes the shot, R denotes receiver and T is the dominate period of the seismic wave. Figure 1 shows a schematic representation of the first Fresnel zone.

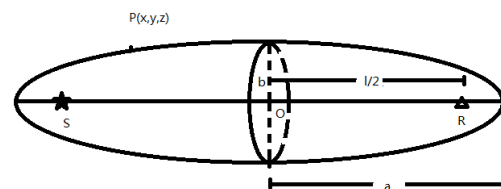


Figure 1: Schematic diagram of the first Fresnel zone.

All the points fall in the volume satisfying equation (1) belong to the first Fresnel zone. For homogeneous media, the first Fresnel zone shows a standard ellipsoid shape and can be easily calculated with given shot and receiver location, dominate frequency of the seismic wave and the

3D wave-ray tomography for near-surface imaging

seismic wave velocity. However, for heterogeneous media, we have to find the first Fresnel zone by multiple raytracings. First, we calculate traveltimes from the shot S to every point P in the model and save the traveltime t_{SP} on every grid points. Then, we calculate traveltimes from the receiver R to every point and save the traveltime t_{RP} . Finally, for each point P, we can use Equation (1) to detect if it is in the first Fresnel zone. From the above procedure, twice forward calculations are required to calculate Fresnel zone for each shot-receiver pair, which significantly increases the computational effort comparing to the first-arrival traveltime tomography. An alternative solution is to store the traveltime field from each receiver to avoid repeated raytracings for overlapped receivers for different shots, but such approach requires tremendous storage space. The computation cost is too high to calculate exact Fresnel zone for 3D seismic exploration applications.

It is important to incorporate the Fresnel zone into 3D traveltime tomography with an efficient method. Here, we propose an efficient approximated first Fresnel zone calculation based on its geometry characteristics. Assuming the velocity model is homogeneous, seismic velocity is v , multiply v to equation (1), we can get

$$|d_{SP} + d_{RP} - d_{SR}| \leq \frac{\lambda}{2} \quad (2)$$

where d denotes distance between two subscript points, and λ is the dominate wavelength. Assuming distance between shot and receiver is l , location of point P is (x, y, z) , equation (2) can be expressed as an ellipsoid function

$$\left[(x-l/2)^2 + r^2 \right]^{1/2} + \left[(x+l/2)^2 + r^2 \right]^{1/2} - l = \frac{\lambda}{2} \quad (3)$$

where $r^2 = y^2 + z^2$ is defined as the Fresnel radius corresponding to a given shot-receiver pair and a specific point P. From equation (3), we can derive some characteristic parameters of this Fresnel ellipsoid:

$$a = \frac{l}{2} \cdot \left(1 + \frac{\lambda}{2l} \right) \quad (4)$$

$$b = \frac{\sqrt{\lambda l}}{2} \cdot \left(1 + \frac{\lambda}{4l} \right)^{\frac{1}{2}} \quad (5)$$

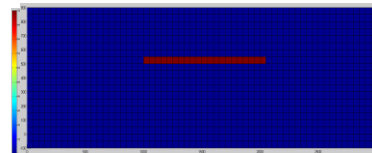
$$r = b \cdot \sqrt{1 - \left(\frac{x}{a} \right)^2} \quad (6)$$

$$\Delta = a - l/2 = \frac{1}{4} \lambda \quad (7)$$

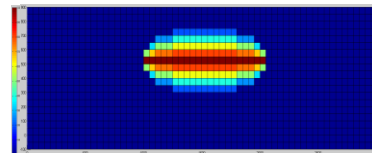
Here, a is the semi-major axis of the ellipsoid, b is the semi-minor axis of the ellipsoid, Fresnel radius r can be expressed by a and b , Δ is the distance between the focus point and the end point, it is called ‘overshooting’ distance (Cerveny and Soares, 1992). For $l \gg \lambda$, overshooting area can be ignored comparing with the whole Fresnel zone.

Based on above quantities, we can approximate the wave ray zone as followings. For each shot-receiver pair, calculate the average velocity along the raypath, store the midpoint of current shot and receiver, calculate a and b by Equation (4) and (5), then we can get wave ray zone after calculating wave ray radius for every point on the raypath with Equation (6). In addition, we define a weighting function to distinguish the capacity of different points in affecting seismic traveltime. Weighting is set 1.0 right on the raypath, and it decreases with distance to raypath, and reduces to zero at the boundary of the wave ray zone. Compared with conventional methods to calculate the exact Fresnel zone, our approach does not need raytracings for each receiver but only the same number of raytracings as the first-arrival traveltime tomography. Figure 2 shows an example of the wave ray calculated by our approach. Figure 2 (a) is the infinite high frequency raypath, Figure 2 (b) - (d) are the wave ray zones along the sections of $x=1500$ m, $y=1500$ m and $z=500$ m, respectively. Our method can reasonably estimate the wave ray zone.

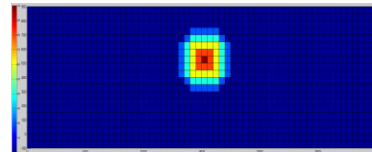
(a) Initial raypath ($x=1500$ m section)



(b) Wave ray zone ($x=1500$ m section)



(c) Wave ray zone ($y=1500$ m section)



3D wave-ray tomography for near-surface imaging

(d) Wave ray zone ($z=500$ m section)

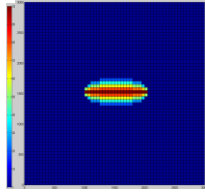


Figure 2: Wave ray zone in a homogeneous model with 3000 m in x direction, 3000 m in y direction, 800 m in z direction, grid size is 50 m. Shot is located at (1500, 1000, 500), receiver is located at (1500, 2000, 500), value on each point is multiplied by 1000 to show wave ray characteristics clearly. (a) Initial ray path; (b) Wave ray zone at $x=1500$ m; (c) Wave ray zone at $y=1500$ m; (d) Wave ray zone at $z=500$ m.

Wave-ray traveltome tomography

Wave-ray tomography is an improved conventional traveltome tomography method. After calculating wave-ray zone of each shot-receiver pair, we apply them to the inversion and make our calculation more physically meaningful; therefore, seismic traveltome is expanded into an integral of traveltome in the wave ray zone.

In order to validate the feasibility of our wave-ray tomography, we do a synthetic test on a 3D near-surface velocity model, which is shown in Figure 4 (a), (d) and (g). The main features of the model are similar to the 2D model in Ke et al., (2007). The scale of the velocity model is 3000 m * 3000 m * 900 m in x, y and z direction, and the grid size is 50 m in each direction. There is a positive gradient in the first layer, with velocity increasing from 1500 m/s to 2400 m/s in the first 450 m in depth, and the second layer starts from $z=500$ m to the bottom of the model, with velocity set at 3500 m/s. Two high velocity anomalies are located just upon the second layer. Both anomalies are 300 m * 400 m * 200 m in each direction with velocity of 3500 m/s, the same as that in the second layer. 36 shots are uniformly distributed at the top of the model, and each shot is recorded by 196 receivers, as shown in Figure 3.

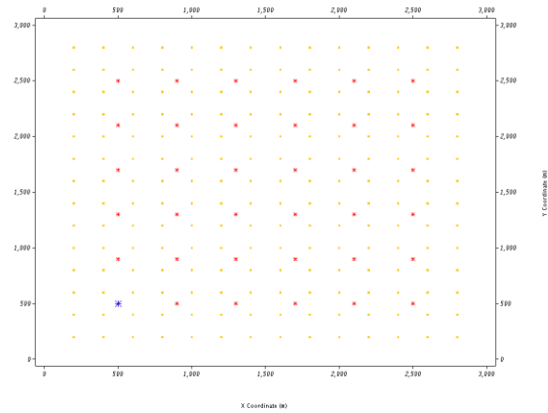
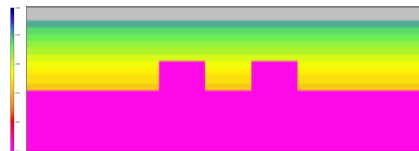


Figure 3: Geometry distribution, in both x and y direction, there are 6 shots and 14 receivers respectively, shot interval is 400 m and receiver interval is 200 m. Red points indicate shots and yellow points represent receivers.

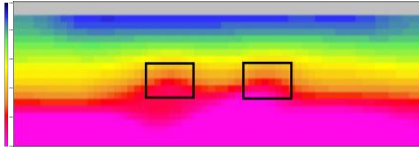
To simulate the real situation, we apply a finite difference calculation on the model with source central frequency 10 Hz, then we pick the first arrivals from the seismogram to obtain observed traveltome. The average reciprocal misfit in the picked traveltome is 50 ms due to the relative low frequency shot wavelet. Then we apply both conventional first-arrival traveltome tomography and wave-ray tomography to the model, and compare the results with true model in Figure 4. Both calculations share the same parameter setting, and the results are derived after 70 iterations. Figure 4 (a), (b) and (c) show $y=1500$ m cross section of these models. It is obvious that Figure 4 (c), which is derived by wave-ray tomography, reveals location and shape more precisely than the conventional tomography result (Figure 4 (b)). Similarly, results of $x=1700$ m and $z=400$ m cross sections, which are shown in Figure 4 (d) to (i), also reveal the advantage of wave-ray tomography over traveltome tomography in detecting anomalies in the near-surface imaging issues. There are some artifacts at the model edge in the results of wave-ray tomography, which is mainly caused by errors in the raypath calculation in such coarse grids. The central frequency selected in the wave-ray tomography is 10 Hz, the same as the central frequency in the forward modeling.

(a) True model $y=1500$ m

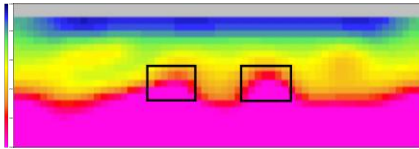


3D wave-ray tomography for near-surface imaging

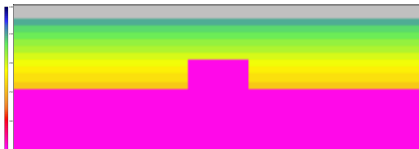
(b) Traveltime tomography $y=1500$ m



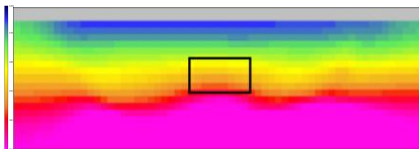
(c) Wave-ray tomography $y=1500$ m



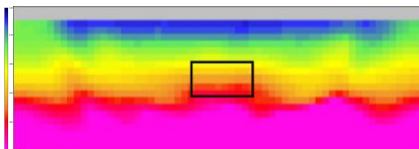
(d) True model $x=1700$ m



(e) Traveltime tomography $x=1700$ m



(f) Wave-ray tomography $x=1700$ m



(g) True model (h) Traveltime tomo (i) Wave-ray tomo

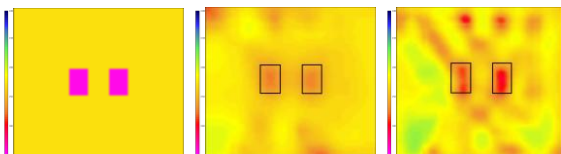


Figure 4: Comparison among true model, traveltime tomography result and wave-ray tomography result. (a), (d) and (g) are three true model cross sections; (b), (e) and (h) are corresponding cross sections of traveltime tomography result; (c), (f) and (i) are

corresponding cross sections of wave-ray tomography. Black rectangles indicate real asperity location.

Both misfits of traveltime tomography and wave-ray tomography reduce to the same level, about 50 ms, close to the traveltime picking error. But these two misfit curves are quite different: in the traveltime tomography, the misfit curve drops very fast and reaches 50 ms after six iterations, and velocity model almost stops updating after then. However, in the wave-ray tomography, the misfit curve reduces relatively slow, and it becomes flat after fifty iterations. That is due to its smoothing nature. From the result comparison, we can see that conventional traveltime tomography is more likely to fall into a local minimal solution, while wave-ray tomography has better capacity in finding the global optimal solution.

Conclusions

In this study, we develop an efficient method to estimate the first Fresnel zone in seismic wave propagation, and implement a wave-ray tomography by introducing an approximate Fresnel zone into 3D first arrival traveltime tomography. Our approach avoids extra raytracing calculation and the high demand for storage space required in the conventional Fresnel volume tomography. Test results on synthetic model confirm the validity of our method.

Acknowledgments

We appreciate GeoTomo providing us the TomoPlus software package to perform this study. We would also like to thank our colleagues for their constructive comments on the study.

<http://dx.doi.org/10.1190/segam2013-0967.1>

EDITED REFERENCES

Note: This reference list is a copy-edited version of the reference list submitted by the author. Reference lists for the 2013 SEG Technical Program Expanded Abstracts have been copy edited so that references provided with the online metadata for each paper will achieve a high degree of linking to cited sources that appear on the Web.

REFERENCES

- Cerveny, V., and J. E. P. Soares, 1992, Fresnel volume ray tracing: *Geophysics*, **57**, 902–915.
- Dahlen, F. A., S. H. Hung, and G. Nolet, 2000, Frechet kernels for finite-frequency traveltimes — I: Theory: *Geophysical Journal International*, **141**, 157–174.
- He, L., J. Zhang, and W. Zhang, 2011, Tradeoffs in the near-surface seismic imaging solutions: 81st Annual International Meeting, SEG, Expanded Abstracts, 4015–4019.
- Husen, S., and E. Kissling, 2001, Local earthquake tomography between rays and waves: fat ray tomography: *Physics of the Earth and Planetary Interiors*, **123**, 127–147.
- Ke, B., J. Zhang, B. Chen, and B. Zhao, 2007, Fat-ray first arrival seismic tomography and its application: 77th Annual International Meeting, SEG, Expanded Abstracts, 2822–2826.
- Luo, Y., and G. T. Schuster, 1991, Wave-equation traveltime inversion: *Geophysics*, **56**, 645–653.
- Tarantola, A., 1984, Inversion of seismic reflection data in the acoustic approximation: *Geophysics*, **49**, 1259–1266.
- Vasco, D. W., J. E. Peterson, and E. L. Majer, 1995, Beyond ray tomography: Wavepaths and Fresnel volumes: *Geophysics*, **60**, 1790–1804.
- Watanabe, T., T. Matsuoka, and Y. Ashida, 1999, Seismic traveltime tomography using Fresnel volume approach: 69th Annual International Meeting, SEG, Expanded Abstracts, 1402–1405.
- Zhang, J., and M. N. Toksoz, 1998, Nonlinear refraction traveltime tomography: *Geophysics*, **63**, 1726–1737.